Characterization of the Causal Interactions Between Depolarization and Repolarization Temporal Changes in Unipolar Electrograms

Michele Orini[1], Luca Citi[2], Ben M Hanson[3], Peter Taggart[1], Pier D Lambiase[1]

[1] Institute of Cardiovascular Science, University College London, UK
[2] School of Computer Science and Electronic Engineering, University of Essex, UK
[3] Dept of Mechanical Engineering, University College London, UK

Abstract

The causes of beat-to-beat cardiac repolarization variability (RV), a marker of electrical instability associated with increased risk of sudden cardiac death, are undetermined. An issue which is often overlooked is whether RV is entirely due to repolarization mechanisms or whether it is partially due to beat-to-beat depolarization variability (DV). To address this issue we propose a methodology to reveal the causal interactions between DV and RV, estimated from unipolar electrograms (EGMs). The methodology is based on the comparison between the coefficients of two autoregressive bivariate models: one describes the actual variabilities, while the other represents the variabilities of surrogate time-series in which directional coupling is selectively destroyed. A simulation study which involves synthetic EGMs generated by using a simplified biophysical model shows that the methodology is accurate in typical conditions. Data from high density, multielectrode, cardiac mapping of the in-vivo human heart recorded in one cardiac patient show that DV drove RV in about 28% of electrodes, suggesting that DV may contribute to RV.

1. Introduction

The cardiac action potential comprises a fast upstroke, which corresponds to a local depolarization, a plateau and a downstroke, which corresponds to a local repolarization. The temporal variability of repolarization (RV) is known to contribute to arrhythmogenesis. In particular, repolarization alternans, RV with frequency equal to 0.5 cycle per beat, is associated with an increased risk of sudden cardiac death [1]. Recent work has shown that repolarization alternans and variability increase before the onset of ventricular arrhythmias in humans [2]. The origin of repolarization alternans/variability is still undetermined, but recent studies show that it may be related to calcium dynamics. An issue which deserves attention, but which is often overlooked, is whether RV is an electrophysiological phenomenon entirely due to repolarization mechanisms or whether it is also due to temporal variability of depolarization (DV) and electrical conduction. In the ECG, repolarization alternans usually manifests in the morphological alternation of the T-wave, while only little variability is observed in the QRS complex, related to depolarization. However, to the extent of our knowledge, this issue was never considered at the cellular or tissue level. To address this issue, in this study we propose a framework based on multivariate autoregressive (AR) analysis to statistically quantify the causal contribution of DV to RV, where surrogate data are used to determine the significance level of the strength of the coupling. Hypothesis tests are used to assess whether DV and RV are characterized by either absence of interactions (DV$\nleftrightarrow$RV), or unidirectional (DV$\rightarrow$RV or DV$\leftarrow$RV), or bidirectional (DV$\leftrightarrows$RV) interactions. We then validate the methodology in a simulation study which involves synthetic unipolar elecrtograms (EGMs), generated by using a simplified biophysical model. Finally, we analyze data from in-vivo electrical cardiac mapping of the human epicardium.

2. Methods

The methodology to describe the causal interactions between DV and RV from EGMs is composed of: (i) Calculation of time-series $x_{\text{D}}(n)$ and $x_{\text{R}}(n)$, representing DV and RV. (ii) Identification of a bivariate AR model, $\mathbf{A}(k)$, which jointly describes $x_{\text{D}}(n)$ and $x_{\text{R}}(n)$, and of two monovariate AR models, $\mathbf{B}_{\text{D}}(k)$ and $\mathbf{B}_{\text{R}}(k)$, which separately describe $x_{\text{D}}(n)$ and $x_{\text{R}}(n)$. (iii) $\mathbf{B}_{\text{D}}(k)$ and $\mathbf{B}_{\text{R}}(k)$ are used to generate surrogate time-series which are characterized by the same structure as $x_{\text{D}}(n)$ and $x_{\text{R}}(n)$ but have no interactions (they only depend on their own history). (iv) Bivariate identification of surrogate series to estimate a threshold value, related to false alarm ratio, above which coefficients indicate that interactions are significant. (v) Hypothesis tests are performed and the structure of the system revealed.

In details, the methodology is as follows: Depolarization

and repolarization intervals, $d(n)$ and $r(n)$, are assumed to fluctuate around a mean value: $d(n) = \overline{d} + x_{\text{D}}(n)$ and $r(n) = \overline{r} + x_{\text{R}}(n)$. They are estimated from the inflection points in the EGMs: $d(n)$ corresponds to the difference between the minimum of the first derivative during depolarization phase and the trigger event (pacing spike during stimulation or atrial activation during sinus rhythm), while $r(n)$ corresponds to the difference between the maximum of the first derivative during the repolarization phase and the trigger event, for both positive and negative T-waves [3] (see Fig. 1). The coefficients of $\mathbf{A}(k)$ are estimated using a least square algorithm [4]:

$$\begin{bmatrix} x_{\text{D}}(n) \\ x_{\text{R}}(n) \end{bmatrix} = \sum_{k=0}^{2} \begin{bmatrix} a_{\text{DD}}(k) & a_{\text{DR}}(k) \\ a_{\text{RD}}(k) & a_{\text{RR}}(k) \end{bmatrix} \begin{bmatrix} x_{\text{D}}(n-k) \\ x_{\text{R}}(n-k) \end{bmatrix} + \begin{bmatrix} \xi_{\text{D}}(n) \\ \xi_{\text{R}}(n) \end{bmatrix} \tag{1}$$

where $\xi_{\text{D}}(n)$ and $\xi_{\text{R}}(n)$, as well as all series denoted as $\xi(n)$ in the following, are IID white Gaussian noise sources. This is an extended model, which takes into account interactions at lag-0 to include the possibility that $x_{\text{D}}(n) \rightarrow x_{\text{R}}(n)$ within the same beat (at $k = 0$ only $a_{\text{RD}}(0) \neq 0$) [4]. The coefficients of $\mathbf{B}_{\text{D}}(k)$ and $\mathbf{B}_{\text{R}}(k)$, $b_{\text{D}}(k)$ and $b_{\text{R}}(k)$, are identified using a least square algorithm:

$$\begin{array}{ll} x_{\text{D}}(n) & = \sum_{k=1}^{2} b_{\text{D}}(k) x_{\text{D}}(n-k) + \xi_{\text{D}}^{\text{M}}(n) \\ x_{\text{R}}(n) & = \sum_{k=1}^{2} b_{\text{R}}(k) x_{\text{R}}(n-k) + \xi_{\text{R}}^{\text{M}}(n) \end{array} \tag{2}$$

Models $\mathbf{B}_{\text{D}}(k)$ and $\mathbf{B}_{\text{R}}(k)$ describe $x_{\text{D}}(n)$ and $x_{\text{R}}(n)$ based on information encoded in their own past (no interaction is assumed in the model) and they can be therefore used to generate surrogate data: time series which share the same structure as $x_{\text{D}}(n)$ and $x_{\text{R}}(n)$ but in which the interactions, if any, have been destroyed. Surrogate time-series, $x_{\text{D}}^{(\text{S})}(n,i)$ and $x_{\text{R}}^{(\text{S})}(n,i)$, where $i = 1, \ldots, 500$ indicate the i-th realization, are generated as:

$$\begin{array}{ll} x_{\text{D}}^{(\text{S})}(n,i) & = \sum_{k=1}^{2} b_{\text{D}}(k) x_{\text{D}}^{(\text{S})}(n-k,i) + \xi_{\text{D}}^{(\text{S})}(n,i) \\ x_{\text{R}}^{(\text{S})}(n,i) & = \sum_{k=1}^{2} b_{\text{R}}(k) x_{\text{R}}^{(\text{S})}(n-k,i) + \xi_{\text{R}}^{(\text{S})}(n,i) \end{array} \tag{3}$$

The coefficients of this bivariate model, $\mathbf{A}^{(\text{S})}(k,i)$, which jointly describes $\{x_{\text{D}}^{(\text{S})}(n,i), x_{\text{R}}^{(\text{S})}(n,i)\}$ are identified using (1). Note that even though $x_{\text{D}}^{(\text{S})}(n,i)$ and $x_{\text{R}}^{(\text{S})}(n,i)$ are independent, the estimated coefficients $a_{\text{DR}}(k)$ and $a_{\text{RD}}(k)$ can be non-zero because they are estimated from noisy, finite length time-series. Threshold values of significance for these coefficients are estimated as the α-percentile of $|a_{\text{DR}}^{(\text{S})}(k,i)|$ and $|a_{\text{RD}}^{(\text{S})}(k,i)|$ and denoted $a_{\text{DR}}^{(\text{S},\alpha)}(k)$ and $a_{\text{RD}}^{(\text{S},\alpha)}(k)$, respectively.

Finally, interactions between DV and RV are determined as follows:

$$\begin{array}{ll} x_{\text{D}} \rightarrow x_{\text{R}} \text{ if} & |a_{\text{RD}}(k)| > a_{\text{RD}}^{(\text{S},\alpha)}(k) \& |a_{\text{DR}}(k)| < a_{\text{DR}}^{(\text{S},\alpha)}(k) \\ x_{\text{D}} \leftarrow x_{\text{R}} \text{ if} & |a_{\text{RD}}(k)| < a_{\text{RD}}^{(\text{S},\alpha)}(k) \& |a_{\text{DR}}(k)| > a_{\text{DR}}^{(\text{S},\alpha)}(k) \\ x_{\text{D}} \leftrightarrows x_{\text{R}} \text{ if} & |a_{\text{RD}}(k)| > a_{\text{RD}}^{(\text{S},\alpha)}(k) \& |a_{\text{DR}}(k)| > a_{\text{DR}}^{(\text{S},\alpha)}(k) \\ x_{\text{D}} \nleftrightarrow x_{\text{R}} \text{ if} & |a_{\text{RD}}(k)| < a_{\text{RD}}^{(\text{S},\alpha)}(k) \& |a_{\text{DR}}(k)| < a_{\text{DR}}^{(\text{S},\alpha)}(k) \end{array}$$

where all the previous relationships are considered true if they hold for at least one lag, i.e. for k =1 or 2 for $a_{\text{DR}}(k)$, and k =0 or 1 or 2 for $a_{\text{RD}}(k)$.

3. Simulation Study

3.1. Synthetic APs and EGMs

Synthetic unipolar EGMs were generated by using the simple model described in [5], derived from the bidomain model assuming that the conductances of the myocardium are isotropic and homogeneous. In this model, an EGM is described as the difference between the local action potential and a position-independent remote component. Cardiac action potentials with controlled depolarization and repolarization intervals were generated using the analytical expressions given in [6], and already used for similar purposes in [7,8]. The framework is described as follows: The transmembrane potentials of $N = 257$ sources (nodes), each one localized at a virtual location $\mathbf{x}$ on the epi- end endocardium, were generated as:

$$V(\mathbf{x},t,n) = a(\mathbf{x}) D(\mathbf{x},t,n) R(\mathbf{x},t,n) - V_0 \tag{4}$$

where for each $\mathbf{x}$, and heart beat n, depolarization and repolarization phases are described by [6]:

$$D(\mathbf{x},t,n) = \frac{1}{1 + e^{-\beta(\mathbf{x})(t - d_{\text{SIM}}(\mathbf{x},n))}}$$

$$R(\mathbf{x},t,n) = \prod_{\text{i}=1}^{2} \left(1 - \frac{1}{1 + e^{-\beta_{\text{i}}(\mathbf{x})(t - r_{\text{SIM}}(\mathbf{x},n))}} \right)$$

where $d_{\text{SIM}}(\mathbf{x},n)$ and $r_{\text{SIM}}(\mathbf{x},n)$ are the depolarization and repolarization times, while $\beta(\mathbf{x})$, $\beta_{\text{1}}(\mathbf{x})$ and $\beta_{\text{2}}(\mathbf{x})$ describe the upstroke during depolarization, and the leading and trailing downslope during repolarization, respectively; $a(\mathbf{x})$ is the amplitude of the transmebrane potential and V_0 is the resting potential. Cycle length is equal to 600 ms, $t \in [0, 600]$. The values of the parameters were obtained by fitting $V(\mathbf{x},t)$ with the transmembrane potential of each node provided by ECGSIM [9] for a normal male. EGM characterized by controlled DV and RV were [5]:

$$S(\mathbf{x},t) = -\frac{g_i}{g_i + g_e} \big(V(\mathbf{x},t) - V_{\text{R}}(t) \big) + w(t) \tag{5}$$

where g_i and g_e are the conductances of intra- and extracellular domain, respectively, and $g_i/(g_i + g_e) = 0.25$ [5], $V_{\text{R}}(t)$ is the position-independent remote component obtained by averaging $V(\mathbf{x},t)$ over all nodes $\mathbf{x}$, and $w(t)$ a white Gaussian noise which accounts for electrical and muscular interferences.

3.2. Validation scheme

Coefficients $\{c_{\text{DD}}(k), c_{\text{DR}}(k), c_{\text{RD}}(k), c_{\text{RR}}(k)\}$, of a bivariate AR model of order 2 which includes lag-0 interactions, $\mathbf{C}(\mathbf{k})$, see (1), are randomly selected from a uniform distribution ranging between -1 and 1. Only those coefficients which correspond to a stable system, i.e. with all poles with magnitude lower than 1, are accepted. Two time series representing DV and RV, $\tilde{x_{\text{D}}}(n)$ and $\tilde{x_{\text{R}}}(n)$, are generated using $\mathbf{C}(\mathbf{k})$, and rescaled to have a controlled standard deviation equal to σ_{D} and σ_{R}. For each node, depolarization and repolarization intervals are estimated as $\tilde{d}(\mathbf{x}, n) = d_{\text{SIM}}(\mathbf{x}, n) + \tilde{x_{\text{D}}}(\mathbf{x}, n)$ and $\tilde{r}(\mathbf{x}, n) = r_{\text{SIM}}(\mathbf{x}, n) + \tilde{x}_{\text{R}}(\mathbf{x}, n)$, and expressions (4)–(5) are used to generate synthetic EGMs.
This configuration is used to simulate the case in which interactions are described by a closed loop ($x_{\text{D}} \rightleftarrows x_{\text{R}}$). The other cases are simulated by using the same procedure but imposing the following conditions:

$$\begin{aligned}
&\text{for } x_{\text{D}} \rightarrow x_{\text{R}} \quad \Longrightarrow c_{\text{DR}}(k) = 0 \text{ for } k = \{1, 2\} \\
&\text{for } x_{\text{D}} \leftarrow x_{\text{R}} \quad \Longrightarrow c_{\text{RD}}(k) = 0 \text{ for } k = \{0, 1, 2\} \\
&\text{for } x_{\text{D}} \nleftrightarrow x_{\text{R}} \quad \Longrightarrow c_{\text{RD}}(k) = 0 \;\&\; c_{\text{DR}}(k) = 0 \; \forall k
\end{aligned}$$

For each of these 4 cases, 257 EGMs are generated and used to assess whether the proposed methodology was able to reveil the underline structure and interactions. The capability of the proposed methodology to correctly determine the type of interaction of the system is quantified in terms of accuracy, i.e. as (TP+TN)/N, being TP and TN the number of true positive and negative detections, and $N = 257$ the number of observations. Furthermore, we study the effect of the amplitude of DV and RV, of sampling frequency and signal to noise ratio on the accuracy of the characterization by varying $\sigma_{\text{D}} = \{1, 2, 3\}$ms, with $\sigma_{\text{R}} = 2\sigma_{\text{D}}$, sampling rate $f_{\text{s}} = \{1, 2\}$ KHz, and SNR $= \{20, 30, 40\}$ dB.

4. Experimental Study

240 epicardial EGM were recorded from a patient undergoing cardiac surgery for coronary artery disease (CABG). Pacing was established from the epicardial left ventricle over a range of 5 cycle lengths, from 600ms to 350ms in steps of 50ms. 30 beats were recorded at each cycle length. DV and RV during the entire protocol were calculated and analyzed as described in the previous section.

5. Results

Figure 1 shows an example of the synthetic signals used in the validation process. Nodes which repolarized earlier (or later) than the remote component, are characterized by positive (or negative) T-waves. Figure 2 shows the accuracy of the proposed methodology in a variety of

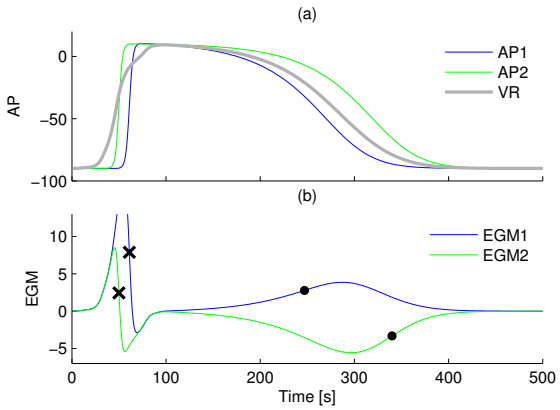

Figure 1. (a) Two local synthetic action potentials and, in bold, the position-independent remote reference. (b) EGM derived as the scaled difference between local action potentials and the remote component. Crosses and circles are depolarization and repolarization times.

situations. From left to right, panels represent results for increasing magnitude of the variability, i.e. σ_{D} and σ_{R}. In each panel, different symbols represent results which correspond to different SNR, and red and blue markers represent results for $f_{\text{s}} = 1$ and 2 KHz, respectively. These results were obtained for a significance level $1 - \alpha = 1\%$. In the application to cardiac mapping, EGMs from 23 electrodes were discarded for being too noisy or due to problems in the detection of the inflection points, and 217 EGMs were analyzed. Among them, interactions $x_{\text{D}} \rightarrow x_{\text{R}}$, $x_{\text{D}} \leftarrow x_{\text{R}}$, $x_{\text{D}} \leftrightarrows x_{\text{R}}$ and $x_{\text{D}} \nleftrightarrow x_{\text{R}}$ were found in 28%, 5%, 13% and 54% of the electrodes, respectively.

6. Discussion

In this study we proposed a methodology to reveal the causal interactions between DV and RV, with the purpose of assessing whether RV is partially due to DV, and to assess whether these causal relationships can be inferred from unipolar EGMs. The methodology is based on the comparison between the coefficients of two bivariate models: the first one describes the actual variabilities, while the other represent the variabilities of surrogate time-series in which the interactions are selectively destroyed.
A simulation study showed that the accuracy of the characterization depended on the amount of variability and on the quality of the signals, and sampling frequency improved the results when the former were lower. For instance, for common conditions, such as $f_{\text{s}} = 1$KHz, SNR $= 30$dB, $\sigma_{\text{DT}} = 2$ms and $\sigma_{\text{RT}} = 4$ms, the interactions DV$\nleftrightarrow$RV, DV$\rightarrow$RV, DV$\leftarrow$RV and DV$\leftrightarrows$RV were detected with an accuracy of 98%, 92%, 82% and 97%, respectively. A similar approach for the generation of synthetic EGMs which

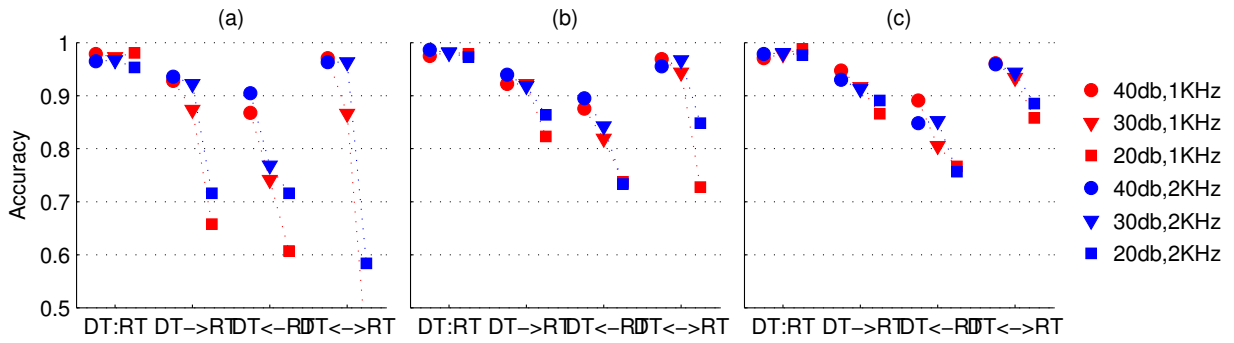

Figure 2. Accuracy in the characterization of the structure of the interactions in the simulation study. From left to right, panels represent results for increasing σ_{D} and σ_{R}. Inside each panel, symbols and color describe the signal to noise ratio, in dB, and the sampling frequency, in KHz (see legend).

correspond to action potentials with controlled depolarization and repolarization intervals has been previously used in [8]. The accuracy for $x_{\mathrm{D}} \leftarrow x_{\mathrm{R}}$ is lower than for the other interactions. This may due to the assumption made in (1) that DV→RV within the same beat.

The analysis of data from in-vivo human cardiac mapping of one patient shows that in about half of the ventricular epicardium RV was independent of DV. However, in more than one fourth of the epicardium RV was driven by DV. In following work, we will assess whether these preliminary results are confirmed in more patients and in sinus rhythm, determine whether DV drives RV also in presence of repolarization alternans, and whether this has an impact on the explanation of such phenomenon.

7. Conclusion

The proposed methodology to characterize activation-repolarization dynamic relationships from EGMs is robust and accurate in typical conditions. Preliminary results have identified where regions of causality occur across one example patient's epicardium, and suggest that DV may contribute to RV.

Acknowledgments

Part of this work has been supported by MRC Project Grant (Ref G0901819).

References

[1] Cutler M, Rosenbaum D. Explaining the clinical manifestations of T wave alternans in patients at risk for sudden cardiac death. Heart Rhythm 2009;6:S22–S28.

[2] Swerdlow C, Chow T, Das M, Gillis A, Zhou X, Abeyratne A, Ghanem R. Intracardiac electrogram T-wave alternans/variability increases before spontaneous ventricular tachyarrhythmias in implantable cardioverter- defibrillator patients: A prospective, multi-center study. Circulation 2011;123(10):1052–1060.

[3] Coronel R, de Bakker JMT, Wilms-Schopman FJG, Opthof T, Linnenbank AC, Belterman CN, Janse MJ. Monophasic action potentials and activation recovery intervals as measures of ventricular action potential duration: experimental evidence to resolve some controversies. Heart Rhythm 2006; 3(9):1043–1050.

[4] Faes L, Nollo G. Biomedical Engineering, Trends in Electronics, Communications and Software. 2011; .

[5] Potse M, Vinet A, Opthof T, Coronel R. Validation of a simple model for the morphology of the T wave in unipolar electrograms. Am J Physiol Heart Circ Physiol Aug 2009; 297(2):H792–H801.

[6] van Dam P, Oostendorp T, Linnenbank A, van Oosterom A. Non-invasive imaging of cardiac activation and recovery. Annals of Biomedical Engineering 2009;37(9):1739–1756.

[7] Sassi R, Mainardi L, Cerutti S. Amplitude of dominant T-wave alternans assessment on ecgs obtained from a biophysical model. Int Conf IEEE EMBS 2011;2011:5872–5875.

[8] Orini M, Hanson B, Taggart P, Lambiase P. Detection of transient, regional cardiac repolarization alternans by time-frequency analysis of synthetic electrograms. Int Conf IEEE EMBS 2013;3773–76.

[9] Van Oosterom A, Oostendorp T. Ecgsim: An interactive tool for studying the genesis of qrst waveforms. Heart 2004; 90(2):165–168.

Address for correspondence:

Name: Michele Orini
Full postal address: 66 Gower st, London, UK
E-mail address: m.orini@ucl.ac.uk